Analysis of Binding Interactions of Pepsin Inhibitor-3 To Mammalian and Malarial Aspartic Proteases†

Rebecca E. Moose,‡ José C. Clemente,‡ Larry R. Jackson,‡ Minh Ngo,‡ Kimberly Wooten,‡ Richard Chang,‡ Antonette Bennett,‡ Sibani Chakraborty,‡ Charles A. Yowell,§ John B. Dame,§ Mavis Agbandje-McKenna,‡ and Ben M. Dunn*,‡

Department of Biochemistry and Molecular Biology, College of Medicine, and Department of Pathobiology, College of Veterinary Medicine, University of Florida, Gainesville, Florida

Received July 25, 2007; Revised Manuscript Received October 10, 2007

ABSTRACT: The nematode *Ascaris suum* primarily infects pigs, but also causes disease in humans. As part of its survival mechanism in the intestinal tract of the host, the worm produces a number of protease inhibitors, including pepsin inhibitor-3 (PI3), a 17 kDa protein. Recombinant PI3 expressed in *E. coli* has previously been shown to be a competitive inhibitor of a subgroup of aspartic proteinases: pepsin, gastricsin and cathepsin E. The previously determined crystal structure of the complex of PI3 with porcine pepsin (p. pepsin) showed that there are two regions of contact between PI3 and the enzyme. The first three N-terminal residues (QFL) bind into the prime side of the active site cleft and a polyproline helix (139−143) in the C-terminal domain of PI3 packs against residues 289−295 that form a loop in p. pepsin. Mutational analysis of both inhibitor regions was conducted to assess their contributions to the binding affinity for p. pepsin, human pepsin (h. pepsin) and several malarial aspartic proteases, the plasmepsins. Overall, the polyproline mutations have a limited influence on the K_i values for all the enzymes tested, with the values for p. pepsin remaining in the low-nanomolar range. The largest effect was seen with a Q1L mutant, with a 200-fold decrease in K_i for plasmepsin 2 from *Plasmodium falciparum* (PfPM2). Thermodynamic measurements of the binding of PI3 to p. pepsin and PfPM2 showed that inhibition of the enzymes is an entropy-driven reaction. Further analysis of the Q1L mutant showed that the increase in binding affinity to PfPM2 was due to improvements in both entropy and enthalpy.

There are over 300 million cases of malaria every year, resulting in at least 1 million deaths annually (World Health Organization, 2006). Malaria is found in tropical and subtropical regions of the world and is caused by one of four species of the plasmodium parasite: *P. falciparum*, *P. vivax*, *P. ovale*, and *P. malariae*. *P. falciparum* is the deadliest of the four species, and *P. vivax* is the most common, responsible for 40−50% of cases in Latin America and Asia.

During the intraerythrocytic stage of the plasmodium parasite's lifecycle in the human host, up to 75% of host cell hemoglobin is degraded (*1*). In *P. falciparum* several proteases have been identified in the food vacuole that are involved in hemoglobin degradation, including a family of aspartic proteases known as the plasmepsins (*2*, *3*). The four plasmepsins found in the food vacuole of *P. falciparum* are PfPM1,[1] PfPM2, PfPM4, and the histoaspartic protease (HAP) (*3*, *4*). It is now believed that the enzymes from *P. vivax* (PvPM4), *P. ovale* (PoPM4), and *P. malariae* (PmPM4) are orthologs of PfPM4 (*5*). Inhibitors of aspartic proteases have been shown to impede growth of the parasite in culture (*3*, *6*−*9*). Therefore, the PfPM4 orthologs would be excellent targets for a single drug therapy directed at all four plasmodium species (*4*).

Most large, proteinaceous inhibitors of aspartic proteases have been isolated from plants (*10*−*20*). For this study, we have analyzed the inhibition of aspartic proteases by a 17 kDa inhibitor known as pepsin inhibitor-3 (PI3), which was originally isolated from the nematode *Ascaris suum* that infects pigs and is closely related to *A. lumbricoides* that infects humans (*21*). Previous studies have found that PI3 is a tight binding inhibitor of pepsin, gastricsin (*21*), and cathepsin E (*22*−*24*).

The structure of PI3 complexed with porcine pepsin (p. pepsin), solved using X-ray crystallography, revealed a unique mode of inhibition (*25*) (Figure 1A). There are two main areas of contact between PI3 and the enzyme. The first three N-terminal residues lie in the prime side of the active site, effectively blocking substrate access. These residues, Gln1, Phe2, and Leu3, correspond to the P1′, P2′, and P3′

† This work is funded by NIH Grants DK18665 and AI39211 to B.M.D.

* To whom correspondence should be addressed. E-mail: bdunn@ufl.edu. Phone: (352) 392-3362. Fax: (352) 846-0412.

‡ College of Medicine.

§ College of Veterinary Medicine.

[1] Abbreviations: PfPM1, *Plasmodium falciparum* plasmepsin 1; PfPM2, *Plasmodium falciparum* plasmepsin 2; PfPM4, *Plasmodium falciparum* plasmepsin 4; PvPM4, *Plasmodium vivax* plasmepsin 4; PoPM4, *Plasmodium ovale* plasmepsin 4; PmPM4, *Plasmodium malariae* plasmepsin 4; HAP, histoaspartic protease; PI3, pepsin inhibitor-3 from *Ascaris suum*; p. pepsin, porcine pepsin; h. pepsin, human pepsin; EDTA, ethylenediaminetetraacetic acid; Nph, nitrophenylalanine.

10.1021/bi7014844 CCC: $37.00
Published on Web 11/16/2007

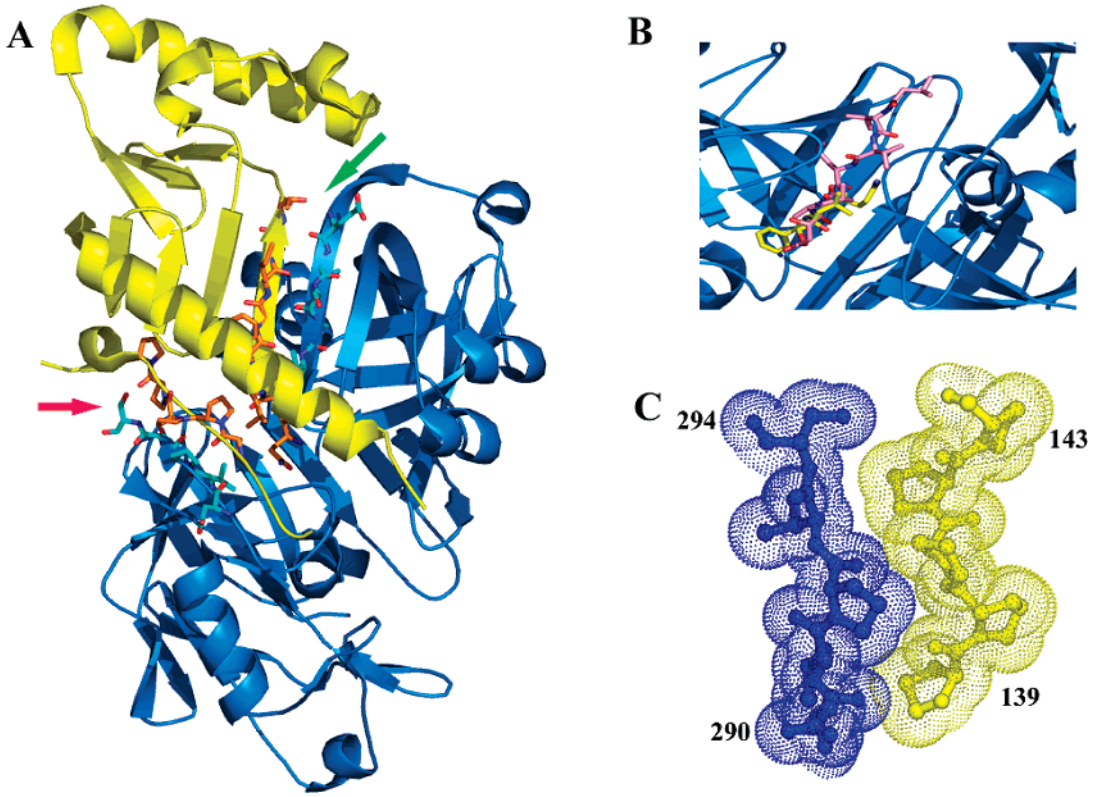

FIGURE 1: (A) Crystal structure of PI3 with p. pepsin (1F34). PI3 is shown by the yellow ribbon and the orange side chains. P. pepsin is shown by the blue ribbon with the cyan side chains. The first eight N-terminal residues of PI3 (green arrow) bind to the enzyme with the first three residues binding into the prime side of the active site and the following five residues forming a β-sheet with the flap of pepsin. The polyproline helix of PI3 (red arrow) packs against the 290s loop of p. pepsin. (B) Close-up of p. pepsin active site with N-terminal residues of PI3 (yellow sticks [1F34]) over pepstatin (pink sticks [1PSO]). (C) Close-up view of polyproline helix (yellow) of PI3 with 290s loop (blue) of p. pepsin (1F34).

positions, respectively (*26*) (Figure 1B). Residues 4−8 of PI3 form hydrogen bonds with residues 70−74 in the flap region of p. pepsin to form an antiparallel β-sheet resulting in an eight-stranded β-sheet spanning both proteins. A polyproline helix in the C-terminal of PI3 is made up of residues 139−143. These residues pack against residues 289−295 (the 290s loop) of p. pepsin (Figure 1C).

Here we describe studies aimed at evaluating the contributions of the sites of interaction between PI3 and p. pepsin to enzyme inhibition, as well as studies to create a better inhibitor for PfPM2 and the PM4 enzymes from all four malarial species. We designed site-specific mutations of the first two N-terminal residues along with several proline to alanine mutations of the polyproline helix of PI3. Dissociation constants of the polyproline mutants of PI3 with p. pepsin, human pepsin (h. pepsin), and PfPM2 showed that this contact region makes a larger contribution to the binding affinity for the pepsins than PfPM2. However, kinetic analysis of the N-terminal mutations of PI3 demonstrated that optimization of this region is crucial to the inhibition of the various plasmepsins. Thermodynamic measurements of PI3 binding to p. pepsin and PfPM2 showed that the interaction was entropically driven. A single mutation to the first residue of PI3 resulted in an improvement in binding to PfPM2 as a result of favorable enthalpy and entropy changes. These observations support the utilization of structure-guided strategies for engineering the inhibitory properties of the naturally occurring PI3 for targeted applications, such as the inhibition of the plasmepsins.

MATERIALS AND METHODS

Expression and Purification. Recombinant PI3 was overexpressed in BL21 DE3 pLysS Star cells grown in LB media supplemented with ampicillin (100 μg/mL) at 37 °C (*25*, *27*). When the OD_{600} reached 0.6, expression was induced by adding 1 mM IPTG, and the cells were allowed to grow for 3 h postinduction. Cells were harvested by centrifugation and resuspended in 4.2 mL/g_{cells} of 50 mM Tris, pH 7.4, 150 mM NaCl, and 1 mM $MgCl_2$. The cells were lysed using a French pressure cell at 1000 psi and subsequently layered over 10 mL of 27% sucrose and centrifuged at 12 500*g* in a swinging bucket rotor for 45 min. The supernatant was discarded, and the pellets were resuspended in 20 mL of 50 mM Tris, pH 7.4, 150 mM NaCl, 1 mM $MgCl_2$, 1% Triton X-100 and centrifuged as before. The resulting pellet contained mostly PI3 and was dissolved in 8 M urea, 300 mM β-mercaptoethanol, 50 mM CAPS, pH 10.5, 1 mM EDTA, 1 mM glycine, and 0.5 M NaCl. The dissolved inclusion bodies were dialyzed against the following buffers: 50 mM Tris, pH 11 (1 h, room temperature), 50 mM Tris, pH 11 (1 h, room temperature), 50 mM Tris, pH 7.5 (5 h, 4 °C), 20 mM MOPS, pH 7.0, 150 mM NaCl (overnight, 4 °C), 20 mM MOPS, pH 7.0, 150 mM NaCl (6 h, 4 °C). Following dialysis, PI3 was further purified by 40% and 70% ammonium sulfate precipitation. PI3, present in the 70% pellet, was dissolved in 100 mM sodium phosphate, pH 5.0, and concentrated before being applied to a Superdex 75 16/60 gel filtration column from Amersham Biosciences for the final stage of purification. All PI3 mutants were created using

the QuikChange mutagenesis kit from Stratagene and expressed and purified as described above.

H. pepsin was also expressed in the form of inclusion bodies, similar to PI3. Inclusion bodies were dissolved in 8 M urea, 50 mM CAPS, pH 10.5, 1 mM EDTA, 1 mM glycine, 500 mM NaCl, and 300 mM β-mercaptoethanol. The protein was refolded by dialyzing against the following buffers: 50 mM Tris (1 h, room temperature), 50 mM Tris, pH 7.5 (12 h, 4 °C), and 20 mM MOPS, 150 mM NaCl, pH 7.0 (6 h, 4 °C). The postdialysate was purified by ion exchange (5 mL HiTrap, Amersham Biosciences) and gel filtration (Superdex 75 16/60, Amersham Biosciences). Lyophilized porcine pepsin was purchased from Sigma-Aldrich and dissolved in 20 mM sodium formate, pH 3.5. The plasmepsins, PfPM2, PfPM4, PoPM4, PmPM4, and PvPM4, were expressed and purified as previously described (*28*).

Kinetic Analysis. K_i values were determined as previously described (*29*, *30*) using chromogenic substrates selected for each enzyme to provide optimal sensitivity in the kinetic assay. The peptide substrates used nitrophenylalanine (Nph) as a reporter group and were synthesized by the University of Florida Protein Core. The substrate used for h. pepsin, PmPM4, PvPM, and PoPM4 was KPIEF*NphRL (* indicates the scissile bond). A derivative of this substrate with an alanine in the P4 position, KAIEF*NphRL, was used with p. pepsin, PfPM2, and PfPM4.

To convert the proenzyme forms to the mature enzyme forms, reactions were preincubated at 37 °C for either 3 min (p. pepsin) or 5 min (h. pepsin and PM2) at the optimum pH for each enzyme (3.5 for the pepsins, 4.4 for the plasmepsins) and cleavage was initiated by mixing with prewarmed substrate. Analysis of the rate data was done with the Enzyme Kinetics module from Sigma Plot. Dissociation constants were also determined at 25 °C for p. pepsin and PfPM2 with the wild-type PI3 and the Q1L mutant for use in calculating thermodynamic properties.

Structure Modeling. Models of PmPM4 and PoPM4 were created using PfPM4 (PDB accession no. 1LS5) as a template in SWISS-MODEL (*31*). Using the least-squares function in O7 (*32*) the known structures of PfPM2 (PDB accession no. 1SME), PfPM4, and PvPM4 (PDB accession no. 1LS5) and the models of PmPM4 and PoPM4 were superimposed onto p. pepsin in the complex with PI3. Individual mutations in PI3 were visualized in silico using PyMol (*33*).

Isothermal Titration Calorimetry. Thermodynamic parameters were determined using a MicroCal VP ITC calorimeter. Experiments were performed with wild-type PI3 and the Q1L mutant with p. pepsin and PfPM2. Inhibitors and enzymes were dialyzed into 10 mM sodium formate, pH 3.5 (p. pepsin) or pH 4.4 (PfPM2). Binding enthalpies were determined for p. pepsin with wild-type PI3 by adding 10 μL injections of inhibitor (100 μM) into the sample cell containing 10 μM enzyme. Determination of binding enthalpies with PfPM2 followed the methods outlined by Nezami et al. (*8*). Briefly, four 10 μL injections of 20−30 μM enzyme were mixed with 100−200 μM inhibitor in the sample cell. This method was adapted for p. pepsin with PI3 Q1L by adjusting the pH to 3.5.

RESULTS

Polyproline Helix Mutations. Alanine substitutions were introduced in the polyproline helix of PI3 to evaluate the individual contribution of each proline during binding, particularly with respect to the need for conformational rigidity. A series of alanine substitutions were made, beginning with the central proline, P141, and extending on either side for combinations of double and triple mutations. Two other single mutants, P140A and P143A, were designed based on the initial kinetic results with the first series of PI3 mutants.

Table 1: K_i Values, in nM, of Wild-Type PI3 and the Polyproline Mutants with P. Pepsin, H. Pepsin, and PfPM2[a,b]

	p. pepsin	h. pepsin	PfPM2
wild-type	0.19 ± 0.04	7.6 ± 0.9	85 ± 9
P141A	0.31 ± 0.08	8.1 ± 1.4	140 ± 20
P140A/P141A	2.8 ± 0.5	48 ± 7	70 ± 8
P141A/P142A	0.53 ± 0.06	15 ± 3	106 ± 10
P139A/P140A/P141A	3.0 ± 0.7	37 ± 6	120 ± 13
P141A/P142A/P143A	6.5 ± 0.8	81 ± 9	60 ± 11
P140A	11 ± 3	42 ± 4	62 ± 12
P143A	1.2 ± 0.3	15.7 ± 0.3	13.8 ± 2.2

[a] All inhibitors are based on the original construct before removal of the N-terminal threonine. [b] P. pepsin, porcine pepsin; h. pepsin, human pepsin; PfPM2, plasmepsin 2 (*Plasmodium falciparum*).

The dissociation constants obtained for wild-type PI3 and the mutants with p. pepsin, h. pepsin, and PfPM2 are shown in Table 1. The wild-type PI3 was a tight binding inhibitor to p. pepsin with a K_i of 0.19 ± 0.04 nM. The P141A and P141A/P142A mutants were also subnanomolar inhibitors of p. pepsin. The K_i values for the P143A, P140A/P141A, P139A/P140A/P141A, P141A/P142A/P143A mutants ranged from 1.2 to 6.5 nM. For p. pepsin, the greatest increase from wild-type in K_i value was observed with P140A (58-fold).

In comparison with the wild-type PI3 binding to p. pepsin, there was a 2-fold increase in K_i for P141A; however, when combined with the P140A mutation, the K_i increased 15-fold. There was no significant change in K_i from P140A/P141A following the addition of P139A. Also, the K_i for P141A/P142A was only 3-fold higher than wild-type; however, the addition of P143A resulted in a 34-fold increase in the K_i value. These results led to the creation of two more single mutants, P140A and P143A, to further analyze the impact of these individual positions on inhibition. The single substitution at Pro140 resulted in a 58-fold increase in K_i compared to wild-type PI3. However, the lack of significant change after addition of P139A to the double mutant P140A/P141A suggests that this proline is not as important for the inhibition of the enzyme. Interestingly, the K_i for the single-mutant P143A was not significantly different from wild-type PI3 for p. pepsin.

Overall, K_i values for wild-type PI3 and the polyproline mutants with h. pepsin were higher than with p. pepsin (Table 1). H. pepsin was not inhibited as tightly as p. pepsin by wild-type PI3 (K_i = 7.6 ± 0.9 nM). Although the P141A mutation had no effect on inhibition, the fold-change from wild-type for the other mutants ranged from 2 to 11.

K_i values were also determined for PfPM2 with the polyproline mutants and, in general, were much higher than for either pepsin (Table 1). Of all the mutations, the single P143A substitution resulted in the greatest decrease in K_i, by 6-fold. Dissociation constants for all of the other polyproline mutants were 1−2-fold higher than wild-type.

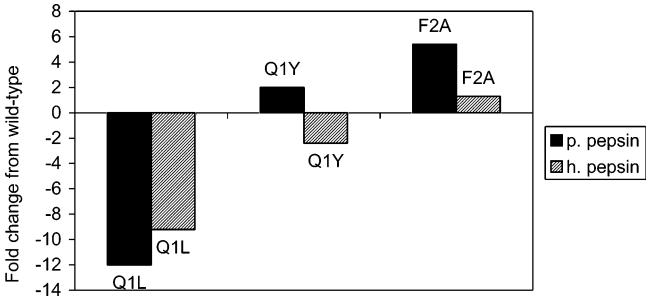

FIGURE 2: Fold-change from wild-type in K_i value of Q1L, F2A, and Q1Y for p. pepsin (solid) and h. pepsin (striped). All inhibitors were based on the construct without the N-terminal threonine.

N-Terminal Mutations. Three PI3 N-terminal residue mutations (Q1L, Q1Y, and F2A) were generated and inhibition constants were determined with p. pepsin, h. pepsin, PfPM2, PfPM4, PoPM4, PmPM4, and PvPM4. The Q1L mutation was designed based on the known cleavage site of PfPM2 at the Phe−Leu bond in the natural hemoglobin substrate (*34*) and combinatorial studies that identified Leu as the most preferred residue at the P1′ position for PfPM2 (*35*). The Q1Y mutation was based on previously determined kinetic data of subsite preferences of PoPM4 (*35*). The F2A mutation, at the P2′ position, was designed based on available structural and kinetic data. First, crystal structures with pepstatin showed that the small side chain of this tight binding inhibitor would be accommodated well by PfPM2. Superposition of the PI3/p. pepsin complex with the PfPM2/pepstatin complex illustrated differences between the active sites of the two enzymes. PfPM2 appeared to have a smaller S2′ pocket than p. pepsin and, therefore, was less likely to accept a large Phe group at this site. Second, previous studies by Westling et al. showed that a synthetic substrate with Ala at the P2′ position was cleaved well by PfPM2 ($k_{cat}/K_m = 438 \pm 30$ mM^{-1} s^{-1}) (*29*).

Before mutations could be made to the N-terminal residues, it was necessary to remove a threonine residue that was added during the initial cloning of the gene (*25*). This Thr was between the starting Met residue and the Gln that is the first residue of the PI3 sequence. The Thr was present in the construct used for crystallization studies, but was not observed in either the crystal structure or N-terminal sequencing of the crystals (*25*), and was most likely cleaved when the enzyme−inhibitor complex was formed. The Thr codon was deleted from the wild-type PI3 using the QuikChange mutagenesis kit (Stratagene), and K_i values were determined for all of the enzymes with this wild-type construct used as a baseline for all of the N-terminal mutants.

Dissociation constants for the interaction of wild-type PI3 and the N-terminal mutants Q1L, F2A, and Q1Y were determined with p. and h. pepsin. These mutants were all tight binding inhibitors, with the highest K_i value being 3.2 nM. The values for all N-terminal mutations are presented as fold-change from wild-type in Figure 2. The F2A and Q1Y mutations had little effect on the inhibition of both pepsins, resulting in 1−5-fold changes compared to the wild-type PI3. The Q1L mutation had the largest effect, lowering the K_i values for p. pepsin and h. pepsin 12- and 9-fold, respectively.

The K_i values for wild-type PI3 and the three mutants, Q1L, F2A, and Q1Y, with the plasmepsins (PfPM2, PfPM4, PoPM4, PvPM4, and PmPM4) are shown in Table 2. Of the five malarial enzymes studied, PfPM2 was the most susceptible to inhibition by wild-type PI3 ($K_i = 20$ nM). Significantly, the Q1L mutation decreased the K_i value for PfPM2 200-fold when compared to wild-type PI3 (Table 2). The K_i values of wild-type PI3 with PoPM4 and PvPM4 were 2−3-fold higher than for PfPM2. PfPM4 and PmPM4 were inhibited the least by wild-type PI3, with K_i values 19- and 14-fold higher than for PfPM2, respectively.

Overall, the F2A substitution had a negative effect on inhibition of the plasmepsins, resulting in higher K_i values for all the plasmepsins, except for PmPM4 which showed a 3-fold decrease from wild-type PI3. For the Q1Y mutation, the K_i value was unchanged for PfPM2 and PvPM4. For PfPM4 and PmPM4 the K_i values decreased by 3- and 7-fold, respectively, compared to wild-type. For PoPM4, the target of this mutation, the K_i value was not significantly different from the wild-type inhibitor.

Isothermal Titration Calorimetry. Binding enthalpies were determined for wild-type PI3 and the Q1L mutant with both p. pepsin and PfPM2. The values of ΔH, ΔG, $-T\Delta S$, and K_i at 25 °C for each enzyme/inhibitor pair are shown in Table 3. The binding enthalpies of p. pepsin with wild-type PI3 and the Q1L mutant differed by only 0.4 kcal mol^{-1}. The K_i values determined at 25 °C were higher than those measured at 37 °C, which corroborates the ITC data showing that this is an endothermic reaction. The binding enthalpy of PfPM2 and the Q1L mutant exhibited a −2 kcal mol^{-1} change from wild-type PI3. The $-T\Delta S$ values for PfPM2 with wild-type PI3 and the Q1L mutant show that the Q1L mutation results in a change of −2.9 kcal mol^{-1}. The $-T\Delta S$ value of p. pepsin with the Q1L mutant changed by 1 kcal mol^{-1} when compared to the wild-type PI3.

The values for ΔCp were also determined for p. pepsin and PfPM2 with wild-type and the Q1L mutant. The Q1L mutation had little effect on ΔCp with p. pepsin. For PfPM2 the ΔCp values decreased from −166 to −650 cal mol^{-1} K^{-1} for wt PI3 and the Q1L mutant, respectively.

DISCUSSION

We have evaluated the effect of mutations within two distinct regions of PI3 on its inhibitory function: the polyproline helix that interacts with the 290s loop of p. pepsin, and the N-terminal region that binds into the prime side of the active site cleft. Multiple effects were observed, depending on the enzyme interactions analyzed.

Polyproline Helix Mutations. The kinetic analysis of the single PI3 mutants, P140A and P143A, with p. pepsin, enabled the contributions of proline positions 140−143 to be better characterized in the context of the double and triple mutants P140A/P141A and P141A/P142A/P143A, respectively. Whereas addition of P140A to P141A resulted in a 15-fold increase in K_i, the single P140A substitution resulted in a 58-fold increase in K_i value compared to wild-type. This suggests that the proline at this position (140) is critical for strong inhibition of p. pepsin. However, the inhibition by the PI3 P143A mutant was not significantly different from that of wild-type PI3, indicating that it is the combination of prolines at positions 141, 142, and 143 which is crucial

Table 2: K_i Values in nM for Wild-Type PI3 and N-Terminal Mutants with PfPM2, PfPM4, PoPM4, PvPM4, and PmPM4[a]

	PfPM2	PfPM4	PvPM4	PmPM4	PoPM4
wild-type	20 ± 3.7	378 ± 50	46 ± 6	282 ± 55	67 ± 12
Q1L	<0.1	3.3 ± 0.4	2.77 ± 0.02	20 ± 2	62 ± 11
Q1Y	25 ± 4	125 ± 31	39 ± 6	42 ± 6	90 ± 12
F2A	175 ± 27	130 ± 17	129 ± 18	76 ± 14	97 ± 16

[a] All mutations to PI3 were added to the construct after removal of the N-terminal threonine.

Table 3: Thermodynamic Parameters for P. Pepsin and PfPM2 with Wild-Type and the Q1L Mutant of PI3[a]

enzyme/inhibitor	ΔG (kcal mol^{-1})	ΔH (kcal mol^{-1})	$-T\Delta S$ (kcal mol^{-1})	K_i (nM)	ΔCp (cal mol^{-1} K^{-1})
p. pepsin/wt	−13.0	12.6	−25.6	0.30 ± 0.04	−824
p. pepsin/Q1L	−13.4	11.2	−24.6	0.14 ± 0.02	−885
PfPM2/wt	−10.4	12.3	−22.7	22 ± 3	−166
PfPM2/Q1L	−12.4	13.2	−25.6	0.8 ± 0.1	−650

[a] All parameters measured at 25 °C.

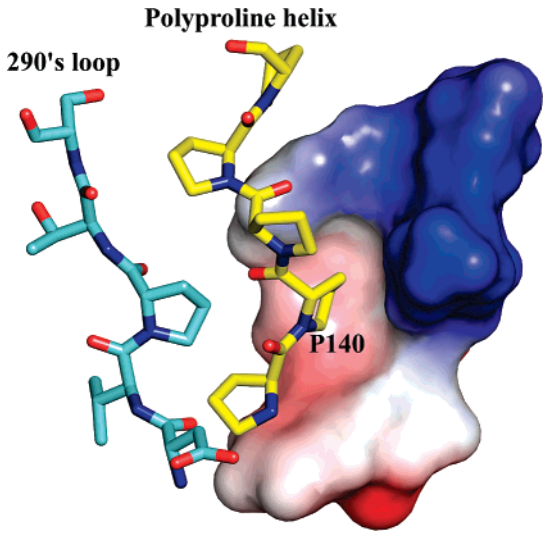

FIGURE 3: Hydrophobic interactions of proline140. The surface of the hydrophobic pocket is shown as an electrostatic potential generated using PyMol 0.99. The pocket is made up of residues T106, F107, K110, I111, and F114. The polyproline helix is shown in yellow. The 290s loop of p. pepsin is shown in blue for orientation (1F34).

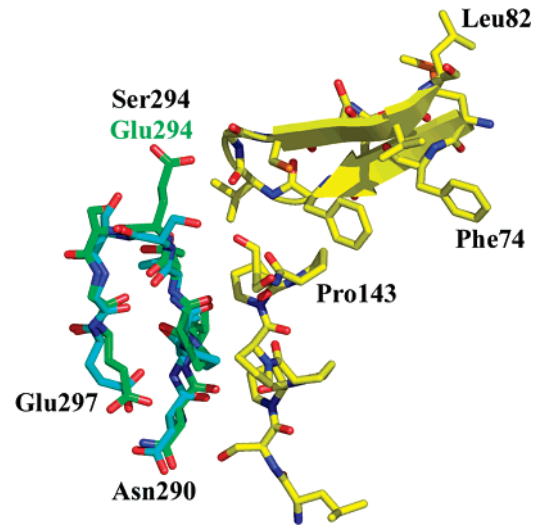

FIGURE 4: Overlap of h. pepsin (1PSO) with PI3/p. pepsin complex (1F34). PI3 is shown in yellow, p. pepsin is in blue, and h. pepsin is in green. Residues labeled in green vary between the two enzymes.

for its optimal binding to p. pepsin. Also, the lack of significant change after addition of P139A to the double mutant P140A/P141A suggests that this proline is not important for binding to the enzyme.

We used molecular modeling to analyze why the single P140A mutation in PI3 would have such an impact on inhibition of p. pepsin. Using the p. pepsin/PI3 complex as a template, Pro140 of PI3 was mutated to alanine in silico using the interactive molecular graphics program O (*32*) and the model was energy minimized and superimposed onto the original template. The side chain of P140 in the wild-type PI3 is pointing away from the 290s loop of p. pepsin and into a hydrophobic pocket in the core of the inhibitor containing residues T106, F107, K110, I111, and F114. The surface potential of this pocket was drawn using the program PyMol (version 0.99) (*33*) and is shown in Figure 3. As a result of the alanine substitution, there is a loss of van der Waals contacts between the side chain of residue 140 and the pocket in the inhibitor, possibly leading to some destabilization of the polyproline helix. This predicted disruption in the polyproline helix could affect its binding contact and interaction with the enzymes and offers a possible explanation for the reduced K_i phenotype observed for the P140A PI3 mutant.

In efforts to explain the difference in the K_i values of PI3 with p. pepsin and h. pepsin, we compared the 3D structures of these enzymes. H. pepsin is 85% identical to p. pepsin in amino acid sequence and has a nearly identical tertiary fold. A superimposition of the structure of h. pepsin (PDB accession no. 1PSO) with the structure of the p. pepsin/PI3 complex (PDB accession no. 1F34) showed that the residues surrounding the N-terminal residues of PI3 were the same in both enzymes. The 290s loop is mostly conserved with only one substitution, glutamate for Ser294 (Figure 4) when comparing p. pepsin and h. pepsin. This residue does not make any direct contact with the polyproline helix of PI3; however, another hairpin-loop in PI3 is ~3 Å away. The change from a small serine side chain to a larger, charged glutamic acid could cause local structural differences in h. pepsin that would affect the conformation of the 290s loop and hence its structural juxtaposition to PI3 residues Phe74 to Leu82, which could affect the overall binding properties of PI3 and h. pepsin.

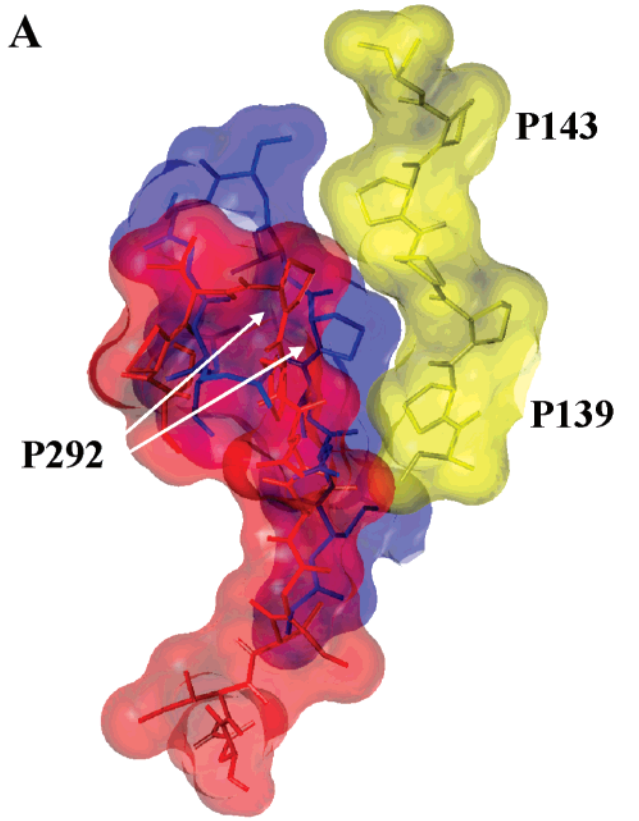

FIGURE 5: Structural and amino acid sequence alignment of 290s loop of PfPM2 with p. pepsin. (A) Polyproline helix of PI3 is shown in the yellow surface (1F34), 290s loop of p. pepsin is in blue (1F34), and the red surface is the homologous loop of PfPM2 (1M43). (B) Amino acid sequence alignment showing deletion in PfPM2 when compared to p. pepsin.

PfPM2 was not inhibited by wild-type PI3 as strongly as p. pepsin or h. pepsin, exhibiting a K_i value of 85 ± 9 nM (Table 2). Changes greater than 10-fold were not observed in the K_i values for any of the polyproline mutations, compared to the wild-type, but the greatest change was a 6-fold decrease in K_i for P143A. Although mutations to the polyproline helix had an overall negative impact on inhibition of the pepsins, these mutations had little effect on the inhibition of PfPM2. These results indicate that the polyproline helix most likely would not interact with PfPM2 in a manner similar to that observed with the pepsins.

The K_i values for the interaction of PI3 with p. pepsin, h. pepsin, and PfPM2 follow the general scheme: $K_i^{\text{p. pepsin}} < K_i^{\text{h. pepsin}} \ll K_i^{\text{PfPM2}}$. Amino acid sequence alignment along with superposition of the structures and models of the plasmepsins onto the p. pepsin/PI3 complex structure allowed us to examine differences in the potential interactions between the inhibitors and PfPM2, compared with the pepsins. There is a striking variation in the structure of PfPM2 in the 290s loop compared to p. pepsin (Figure 5). The structural alignment shows that this loop is truncated in PfPM2 and most likely would not fully contact the polyproline helix of PI3. Significantly, introducing structural flexibility in this region of PI3 (P143A mutant) decreases the interaction with PfPM2 compared to that of the wild-type inhibitor.

N-Terminal Mutations. K_i values for wild-type PI3 and the three mutants, Q1L, F2A, and Q1Y, were determined for the plasmepsins. All of these enzymes have been shown by an analysis using a combinatorial substrate library (*35*) to have a low affinity for Gln in the P1′ position. Overall, these enzymes more readily accepted Leu at this position in previous studies, and the results obtained in this study support this assertion. The substitution of Gln1 with Leu greatly decreased the K_i for PfPM2 (200-fold), PfPM4 (114-fold), PvPM4 (16-fold), and PmPM4 (14-fold). Inhibition by the mutant Q1L was essentially the same as the wild-type PI3 for PoPM4. PoPM4 varied from the other PfPM4 orthologs in that Leu was only marginally accepted at the P1′ position in the combinatorial substrate library study (*35*). A Tyr substitution was designed to target PoPM4 specifically. However, the Q1Y mutation did not significantly affect the inhibition of any of the malarial enzymes, including PoPM4 when compared to wild-type PI3. The largest effect was seen with PmPM4, which had a 7-fold decrease in K_i value.

The F2A substitution in PI3 did not result in any significant decrease in K_i values for the malarial enzymes. This mutation resulted in a 9-fold increase in the K_i value for PfPM2. For the other malarial enzymes, the K_i values for the F2A mutant were no more than 3-fold higher or lower than wild-type. Current structural and substrate studies are consistent with the results of the F2A mutant (*35*). The structure of the uncomplexed PfPM2 revealed that the active site of PfPM2 is larger than commonly assumed based on structures of the enzyme in complex with inhibitors (*36*). The enzyme appears to be extremely flexible and is able to accommodate a variety of different structures in the active site, particularly in the S2′ pocket. Also, the Phe residue would form more substantial hydrophobic interactions with the enzyme than Ala.

Potential binding between PfPM2 and the N-terminal residues of PI3 was analyzed by superimposing the known structure of PfPM2, complexed with pepstatin, (PDB accession no. 1M43) onto the p. pepsin/PI3 complex (PDB accession no. 1F34). It is known from substrate preference studies that PfPM2 has different subsite preferences than the pepsins, which was the rationale utilized for generating the Q1L mutant. The observed decrease in K_i value for the Q1L mutant and PfPM2 was consistent with an improved interaction between the inhibitor and enzyme, given that this enzyme has a preference for Leu in the P1′ site. Visual analysis of the residues in p. pepsin and the plasmepsins that are within 4 Å of the N-terminal residues of PI3 shows that many of these residues are conserved. However, there are variations at positions 73, 74, 76, 128, and 289 (pepsin numbering). In general, these are conservative substitutions; however, the difference at position 74 is significant in PoPM4, which is the only plasmepsin lacking a polar residue (Figure 6). The pocket of PI3 that surrounds residue 74 has a negative surface charge that would likely be incompatible with the hydrophobic leucine of PoPM4 providing a potential explanation for the reduced inhibitory effect of PI3 on this enzyme.

Isothermal Titration Calorimetry. The positive, unfavorable, enthalpy values (Table 3) observed for the binding of

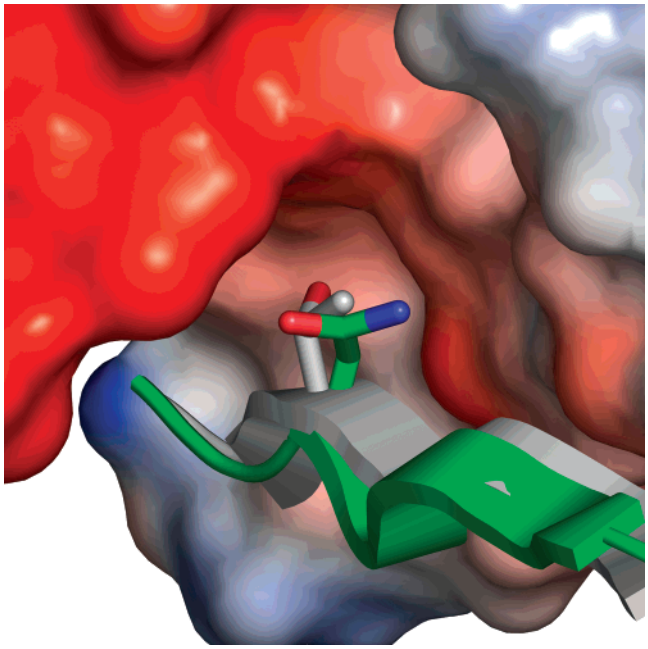

FIGURE 6: Charged pocket surrounding Thr74 of p. pepsin, white ribbon and stick (1F34). The corresponding Asn76 of PfPM2 is shown in green (1M43). The surface of the pocket is shown as an electrostatic potential generated using PyMol 0.99.

PI3 to pepsin and PfPM2 show that these enzyme−inhibitor interactions are driven primarily by changes in entropy. This suggests that hydrophobic interactions provide the main contribution to binding. There was a small decrease in K_i value for p. pepsin when comparing the Q1L mutant to wild-type PI3. This is a result of a 1.5 kcal mol^{-1} decrease in binding enthalpy that compensates for an unfavorable change in entropy ($-T\Delta\Delta S$ of 1 kcal mol^{-1}). There was very little difference in the ΔCp values for p. pepsin with the wild-type and mutant inhibitors. From this we can conclude that there is very little change in the buried surface area during binding of both the wild-type PI3 and Q1L mutant to p. pepsin (*37*). Therefore, it is reasonable to expect that the overall binding interactions of the mutant inhibitor are similar to the wild-type inhibitor with p. pepsin.

The Q1L mutation in PI3 had a much larger effect on the interactions with PfPM2. The heat capacity change was altered substantially in the negative direction, 484 cal mol^{-1} K^{-1}. This indicates a large increase in water displacement upon binding of the Q1L mutant compared to wild-type PI3. This is supported by an increase in enthalpy (0.9 kcal mol^{-1}) and an increase in entropy ($-T\Delta\Delta S$ of -2.9 kcal mol^{-1}) indicating an increase in hydrophobic interactions between PI3 Q1L and PfPM2 when compared to wild-type PI3. Experimentally, it has been shown that a Gln to Leu substitution is accompanied by a ΔCp of approximately 215 cal mol^{-1} K^{-1} (*38*). The large change in heat capacity observed with the Q1L mutant suggests that this single substitution may affect binding interactions in regions other than the active site, resulting in tighter binding to PfPM2 compared to the wild-type.

CONCLUSIONS

The polyproline helix and the N-terminal residues of PI3 were both observed to be important for inhibition of various aspartic proteases. The polyproline helix is very important for inhibition of the pepsins, but not the plasmepsins, consistent with the prediction that it will not make many significant contacts with these enzymes. However, it is interesting that replacing the most C-terminal proline with an alanine (P143A) led to stronger inhibition of PfPM2. This added flexibility may be a site for future study in attempts to improve inhibition of PfPM2 with PI3.

The kinetic data for the N-terminal mutants of PI3 illustrated that the side chains of these residues are very important for inhibition by PI3. The Q1L mutation had a significant effect on inhibition of h. and p. pepsin, although the greatest effect was the 200-fold decrease in K_i value for PfPM2. This result is notable not simply for the decrease in K_i value but because it appears that this mutation outweighed the lack of optimal shape complementarity at the 290s loop in PfPM2 with P13, as shown by the thermodynamic results. The F2A mutation also verified the importance of the N-terminal residues; placement of the less-preferred phenylalanine at the P2′ position for PfPM2 proved to be significantly deleterious to inhibition, highlighting the importance of favorable interactions in the region. These results indicate that although the polyproline helix is a required element for inhibition of the pepsins and related enzymes, in the absence of strong interactions, as with the malarial enzymes, the N-terminal residues of PI3 become even more influential in binding of the inhibitor.

ACKNOWLEDGMENT

The authors thank Robert McKenna, Ph.D., Bret B. Beyer, Ph.D. and Katie Clifford for their help with this study.

REFERENCES

1. Goldberg, D. E., Slater, A. F., Cerami, A., and Henderson, G. B. (1990) Hemoglobin degradation in the malaria parasite *Plasmodium falciparum*: an ordered process in a unique organelle, *Proc. Natl. Acad. Sci. U.S.A. 87*, 2931−2935.
2. Hill, J., Tyas, L., Phylip, L. H., Kay, J., Dunn, B. M., and Berry, C. (1994) High level expression and characterisation of plasmepsin II, an aspartic proteinase from *Plasmodium falciparum*, *FEBS Lett. 352*, 155−158.
3. Francis, S. E., Gluzman, I. Y., Oksman, A., Knickerbocker, A., Mueller, R., Bryant, M. L., Sherman, D. R., Russell, D. G., and Goldberg, D. E. (1994) Molecular characterization and inhibition of a *Plasmodium falciparum* aspartic hemoglobinase, *EMBO J. 13*, 306−317.
4. Banerjee, R., Liu, J., Beatty, W., Pelosof, L., Klemba, M., and Goldberg, D. E. (2002) Four plasmepsins are active in the *Plasmodium falciparum* food vacuole, including a protease with an active-site histidine, *Proc. Natl. Acad. Sci. U.S.A. 99*, 990−995.
5. Dame, J. B., Yowell, C. A., Omara-Opyene, L., Carlton, J. M., Cooper, R. A., and Li, T. (2003) Plasmepsin 4, the food vacuole aspartic proteinase found in all *Plasmodium* spp. infecting man, *Mol. Biochem. Parasitol. 130*, 1−12.
6. Haque, T. S., Skillman, A. G., Lee, C. E., Habashita, H., Gluzman, I. Y., Ewing, T. J., Goldberg, D. E., Kuntz, I. D., and Ellman, J. A. (1999) Potent, low-molecular-weight non-peptide inhibitors of malarial aspartyl protease plasmepsin II, *J. Med. Chem. 42*, 1428−1240.
7. Jiang, S., Prigge, S. T., Wei, L., Gao, Y., Hudson, T. H., Gerena, L., Dame, J. B., and Kyle, D. E. (2001) New class of small nonpeptidyl compounds blocks *Plasmodium falciparum* development in vitro by inhibiting plasmepsins, *Antimicrob. Agents Chemother. 45*, 2577−2584.
8. Nezami, A., Luque, I., Kimura, T., Kiso, Y., and Freire, E. (2002) Identification and characterization of allophenylnorstatine-based inhibitors of plasmepsin II, an antimalarial target, *Biochemistry 41*, 2273−2280.

9. Rosenthal, P. J. (1995) *Plasmodium falciparum*: effects of proteinase inhibitors on globin hydrolysis by cultured malaria parasite, *Exp. Parasitol. 80*, 272−281.
10. Phylip, L. H., Lees, W. E., Brownsey, B. G., Bur, D., Dunn, B. M., Winther, J. R., Gustchina, A., Li, M., Copeland, T., Wlodawer, A., and Kay, J. (2001) The potency and specificity of the interaction between the IA(3) inhibitor and its target aspartic proteinase from *Saccharomyces cerevisiae*, *J. Biol. Chem. 276*, 2023−2030.
11. Li, M., Phylip, L. H., Lees, W. E., Winther, J. R., Dunn, B. M., Wlodawer, A., Kay, J., and Gustchina, A. (2000) The aspartic proteinase from *Saccharomyces cerevisiae* folds its own inhibitor into a helix, *Nat. Struct. Biol. 7*, 113−117.
12. Keilova, H., and Tomasek, V. (1976) Isolation and some properties of cathepsin D inhibitor from potatoes, *Collect. Czech. Chem. Commun. 41*, 489−497.
13. Mares, M., Meloun, B., Pavlik, M., Kostka, V., and Baudys, M. (1989) Primary structure of cathepsin-D inhibitor from potatoes and its structure relationship to soybean trypsin-inhibitor family, *FEBS Lett. 251*, 94−98.
14. Ritonja, A., Krizaj, I., Mesko, P., Kopitar, M., Lucovnik, P., Strukelj, B., Pungercar, J., Buttle, D. J., Barrett, A. J., and Turk, V. (1990) The amino acid sequence of a novel inhibitor of cathepsin D from potato, *FEBS Lett. 267*, 13−15.
15. Hannapel, D. J. (1990) Differential expression of potato-tuber protein genes, *Plant Physiol. 94*, 919−925.
16. Werner, R., Guitton, M. C., and Muhlbach, H. P. (1993) Nucleotide-sequence of a cathepsin-D inhibitor protein from tomato, *Plant Physiol. 103*, 1473−1473.
17. Farley, P. C., Christeller, J. T., Sullivan, M. E., Sullivan, P. A., and Laing, W. A. (2002) Analysis of the interaction between the aspartic peptidase inhibitor SQAPI and aspartic peptidases using surface plasmon resonance, *J. Mol. Recognit. 15*, 135−144.
18. Wilhite, S. E., Elden, T. C., Puizdar, V., Armstrong, S., and Smigocki, A. C. (2000) Inhibition of aspartyl and serine proteinases in the midgut of sugarbeet root maggot with proteinase inhibitors, *Entomol. Exp. Appl. 97*, 229−233.
19. Galleschi, L., Friggeri, M., Repiccioli, R., and Come, D. (1993) Aspartic proteinase inhibitor from wheat: some properties. In *Proceedings of the Fourth International Workshop of Seeds: Basic and Applied Aspects of Seed Biology* (Come, D. and Corbineau, F., Eds.) pp 207−211, ASFIS, Paris.
20. Lenarcic, B., and Turk, V. (1999) Thyroglobulin type-1 domains in equistatin inhibit both papain-like cysteine proteinases and cathepsin D, *J. Biol. Chem. 274*, 563−566.
21. Abu-Erreish, G. M., and Peanasky, R. J. (1974) Pepsin inhibitors from *Ascaris lumbricoides*−Isolation, purification, and some properties, *J. Biol. Chem. 249*, 1558−1565.
22. Jupp, R. A., Richards, A. D., Kay, J., Dunn, B. M., Wyckoff, J. B., Samloff, I. M., and Yamamoto, K. (1988) Identification of the aspartic proteinases from human erythrocyte membranes and gastric mucosa (slow-moving proteinase) as catalytically equivalent to cathepsin E, *Biochem. J. 254*, 895−898.
23. Keilova, H., and Tomasek, V. (1972) Effect of pepsin inhibitor from *Ascaris lumbricoides* on cathepsin D and E, *Biochim. Biophys. Acta 284*, 461−464.
24. Samloff, I. M., Taggart, R. T., Shiraishi, T., Branch, T., Reid, W. A., Heath, R., Lewis, R. W., Valler, M. J., and Kay, J. (1987) Slow moving proteinase. Isolation, characterization, and immunohistochemical localization in gastric mucosa, *Gastroenterology 93*, 77−84.
25. Ng, K. K. S., Petersen, J. F. W., Cherney, M. M., Garen, C., Zalatoris, J. J., Rao-Naik, C., Dunn, B. M., Martzen, M. R., Peanasky, R. J., and James, M. N. G. (2000) Structural basis for the inhibition of porcine pepsin by *Ascaris* pepsin inhibitor-3, *Nat. Struct. Biol. 7*, 653−657.
26. Schechter, I., and Berger, A. (1968) On active site of proteases. 3. Mapping active site of papain−specific peptide inhibitors of papain, *Biochem. Biophys. Res. Commun. 32*, 898−902.
27. Zalatoris, J., Rao-Naik, C., Fecho, G., Girdwood, K., Kay, J., and Dunn, B. M. (1998) Expression, purification, and characterization of the recombinant pepsin inhibitor from *Ascaris suum*, *Adv. Exp. Med. Biol. 436*, 387−389.
28. Westling, J., Yowell, C. A., Majer, P., Erickson, J. W., Dame, J. B., and Dunn, B. M. (1997) *Plasmodium falciparum*, *P. vivax*, and *P. malariae*: a comparison of the active site properties of plasmepsins cloned and expressed from three different species of the malaria parasite, *Exp. Parasitol. 87*, 185−193.
29. Westling, J., Cipullo, P., Hung, S. H., Saft, H., Dame, J. B., and Dunn, B. M. (1999) Active site specificity of plasmepsin II, *Protein Sci. 8*, 2001−2009.
30. Dunn, B. M., Scarborough, P. E., Davenport, R., and Swietnicki, W. (1994) Analysis of proteinase specificity by studies of peptide substrates. The use of UV and fluorescence spectroscopy to quantitate rates of enzymatic cleavage, *Methods Mol. Biol. 36*, 225−243.
31. Schwede, T., Kopp, J., Guex, N., and Peitsch, M. C. (2003) SWISS-MODEL: An automated protein homology-modeling server, *Nucleic Acids Res. 31*, 3381−3385.
32. Jones, T. A., Zou, J. Y., Cowan, S. W., and Kjeldgaard. (1991) Improved methods for building protein models in electron density maps and the location of errors in these models, *Acta Crystallogr., Sect. A 47 (Part 2)*, 110−119.
33. DeLano, W. L. (2002). The PyMol Molecular Graphics System. DeLano Scientific, Palo Alto, CA, www.pymol.org.
34. Goldberg, D. E., Slater, A. F., Beavis, R., Chait, B., Cerami, A., and Henderson, G. B. (1991) Hemoglobin degradation in the human malaria pathogen *Plasmodium falciparum*: a catabolic pathway initiated by a specific aspartic protease, *J. Exp. Med. 173*, 961−969.
35. Beyer, B. B., Johnson, J. V., Chung, A. Y., Li, T., Madabushi, A., Agbandje-McKenna, M., McKenna, R., Dame, J. B., and Dunn, B. M. (2005) Active-site specificity of digestive aspartic peptidases from the four species of *Plasmodium* that infect humans using chromogenic combinatorial peptide libraries, *Biochemistry 44*, 1768−1779.
36. Asojo, O. A., Gulnik, S. V., Afonina, E., Yu, B., Ellman, J. A., Haque, T. S., and Silva, A. M. (2003) Novel uncomplexed and complexed structures of plasmepsin II, an aspartic protease from *Plasmodium falciparum*, *J. Mol. Biol. 327*, 173−181.
37. Pierce, M. M., Raman, C. S., and Nall, B. T. (1999) Isothermal titration calorimetry of protein−protein interactions, *Methods 19*, 213−221.
38. Loladze, V. V., Ermolenko, D. N., and Makhatadze, G. I. (2001) Heat capacity changes upon burial of polar and nonpolar groups in proteins, *Protein Sci. 10*, 1343−1352.

BI7014844